

Supercritical Antisolvent Precipitation of Quercetin Systems: Preliminary Experiments

P. Alessi,^a A. Cortesi,^a N. De Zordi,^{a,*} T. Gamse,^c I. Kikic,^a M. Moneghini,^b and D. Solinas^a

^aDepartment of Engineering and Architecture,
University of Trieste, Via Valerio 10, 34127 Trieste, Italy

^bDepartment of Chemical and Pharmaceutical Sciences,
University of Trieste, P.le Europa 1, 34127 Trieste, Italy

^cInstitut für Chemische Verfahrenstechnik und Umwelttechnik,
Technische Universität Graz, Inffeldgasse 25/C/IIA.8010, Graz

Original scientific paper

Received: June 12, 2012

Accepted: July 25, 2012

Flavonoids have attracted a lot of attention due to their antioxidant, antitumor and antibacterial activities. Quercetin (3,5,7,3,4-pentahydroxyflavone) is a polyphenolic flavonoid that shows several biological effects including a strong inhibitory effect on the growth of several human and animal cancer cell lines and enhances the antiproliferative effect of cisplatin both in-vitro and in-vivo. In spite of a variety of its biological effects, Quercetin is very poorly soluble in water, which has limited its absorption upon oral administration.

As known, the solubility of drug is often due to the increase of the surface/volume ratio which implies the increase of the number of surface atoms (or molecules) with respect to the number of bulk atoms (or molecules). With this aim, we investigated the use of supercritical antisolvent (SAS) technique for Quercetin microparticles generation finding the best operative conditions through the Peng Robinson's Equation of State.

The obtained simulation behaviors were confirmed by experimental precipitation: the physicochemical characterizations of the samples were also performed.

Key words:

Quercetin, supercritical antisolvent technique, micronisation, physicochemical characterization

Introduction

Quercetin (Quer) is one of several naturally-occurring flavonol compounds belonging to the broader group of polyphenolic flavonoid substances, which are characterized by a phenyl benzo(y)pyrone-derived structure consisting of 2 benzene rings linked by a heterocyclic pyran ring^{1,2}. These compounds have been reported to exhibit strong antioxidant properties³ and fruits and vegetables (particularly onions and apples) were identified as the primary sources of dietary Quercetin⁴⁻⁶. Black tea also was identified as a rich dietary source of Quercetin^{7,8}. National (e.g., Australia, the Netherlands, Finland, Italy, Croatia, Japan, United States) dietary record-based cohort assessments of the intake of Quercetin from the habitual diet indicated consumption levels of up to approximately 40 mg Quercetin/day⁹⁻¹³. Dietary Quercetin is metabolized in the intestine and liver, and gradually accumulates in the liver and then in the kidney and other organs¹⁴⁻¹⁶. Thus, the liver might be a major organ

affected by habitual consumption of a Quercetin-rich diet.

In spite of a variety of its biological effects, Quer is very poorly soluble in water, which has limited its absorption upon oral administration.

Oral bioavailability of a drug depends on its solubility and/or dissolution rate, and dissolution can be the rate limiting step for the onset of therapeutic activity¹⁷.

Literature reports many strategies to improve its bioavailability like salt formation, co-crystallization, complexation, prodrug, lyophilization (freeze drying), liposome preparation, spray drying technologies, adding solvents or surface active agents, solid dispersions formation and micronization¹⁸⁻²³.

The basic principle of the micronization is to increase the dissolution rate by increasing the surface area. This process includes the intensive techniques like milling²⁴, freeze drying²⁵ and spray-drying²⁶, or recrystallizing the particles from solutions and sometimes playing (when possible) on the different polymorphic forms²⁷⁻²⁹. Problems with these last traditional methods include the use of large

*Corresponding author: ndezordi@units.it Phone: +39 040553105 Fax: +3904052572

amounts of solvent, solvent residues, broad particle size distributions, as well as a thermal and chemical degradation of the products.

Recently, the supercritical anti-solvent (SAS) process has been proposed as an alternative method either to prepare coprecipitate (that may be smaller in particle size, lower in residual organic solvents and with a better flowability) or to micronize. In the SAS process, a supercritical fluid is used as anti-solvent, causing the precipitation of the substrates initially dissolved in a liquid solvent. The modification of solid state characteristics such as crystal habit, crystallinity, and polymorphism has gained increasing attention in pharmaceutical research and has been successfully achieved through the precipitation of drug particles using various SAS processes^{30–39}. In particular, supercritical fluids (SCF) process operating parameters can be adjusted to vary supersaturation and conditions for nucleation and crystal growth across a wide range. Accordingly, the different forms of a compound in which the molecules have different arrangements and/or conformations can be controlled using the SAS process. Polymorphic and amorphous forms usually exhibit different physicochemical properties, including dissolution performance^{27–29}.

The present study aims to improve the dissolution rate of Quercetin by SAS method from three different polar solvents: acetone, ethanol (EtOH) and dimethylsulfoxide (DMSO). Moreover the Peng Robinson's Equation of State (PR-EoS), with interaction parameters calculated from binary solubility data, is applied to describe the ternary systems (Quer, solvent and CO₂) in the SAS experiments.

The physicochemical characterizations through powder X-ray diffraction, optical microscopy and DRIFT spectroscopy were carried out to understand the influence of the adopted technological process on the physical status of drug. In addition, the dissolution tests of the Quercetin in the considered systems were also discussed.

Materials and methods

Quercetin dihydrate and CO₂ (purity 99.9%) were purchased from Galeno (Italy) and Siad (Italy) respectively. All the solvents (acetone, ethanol and dimethylsulfoxide) were of analytical grade and were provided by J.T. Baker (Netherlands).

Determination of Quercetin solubility in organic solvents

Quercetin solubility (table 1) in the organic solvents was measured at 299.0, 303.0, 308.0 and 313.0 K. Weighted amount of the drug were added

Table 1 – Experimental molar fraction solubility x of Quercetin in the considered organic solvents

Solvent	$T(K)$	$10^2 x$
Acetone	299.0	0.005
	303.0	0.007
	308.0	0.015
	313.0	0.021
Ethanol	299.0	0.030
	303.0	0.032
	313.0	0.049
DMSO	299.0	0.607
	303.0	0.634
	313.0	0.666

to 10 mL of solvent, under stirring conditions, until turbidity was observed. The solutions were then filtered after a time of equilibration: it was verified that stable conditions were reached in about one hour. The concentrations were then evaluated spectrophotometrically (Thermo Scientific Evolution 60 S, USA). Each experiment was carried out in triplicate with a coefficient of variation (CV) less than 3%, as reported by Kikic et al.⁴⁰.

SAS method

A schematic diagram of SAS equipment used in this study is reported in Figure 1.

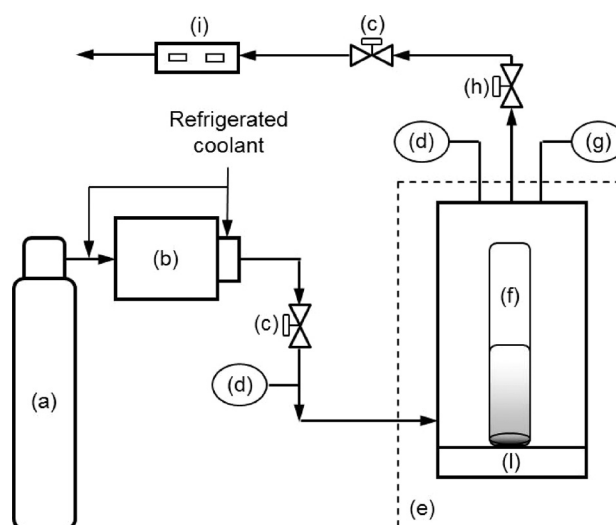


Fig. 1 – SAS equipment: a) CO₂ Cylinder, b) CO₂ Pump, c) On-Off valve, d) P transducers, e) Air oven, f) HP View cell, g) T probe, h) Lamination valve, i) Flow meter, l) Magnetic stirrer

A 150 cm³ precipitator vessel (AISI-316 steel) with a sapphire visual cell was filled with 5 ml of Quer saturated solution in organic solvent. The vessel was placed in an water bath ensuring temperature to be kept within ± 0.5 K.

Liquid CO₂ was fed from the bottom of the precipitator by a high pressure pump (Lewa EK-M-210V1) and then stirred, in the vessel, at 250 rpm with a magnetic stirrer.

When the liquid phase expanded, for the CO₂ anti-solvent effect, the formed particles were retained in the vessel. To allow the elimination of the organic solvent and the recovery of dry particles the apparatus was then employed in dynamic way: the outlet flow was filtered (0.22 μ m) to prevent precipitate losses and regulated by a heated metering valve (Whitey SS-21RS4) at 1 L·min⁻¹.

Temperature and pressure values in the precipitator were measured by a PT100 thermometer (HD 9214, ± 0.1 K) and a JUMO pressure transducer (DPI 260, ± 0.1 bar), respectively. Each precipitation experiment was carried out in triplicate.

Solubility calculations

The knowledge of the Quercetin solubility as a function of the solvent and anti-solvent composition is essential to describe, with a model, the experimental conditions for the antisolvent precipitation process.

The phase equilibrium of a pure solid (component 3) in a solution of composition x_3 can be described by the following equilibrium equation:

$$f_3^S(T, P) = x_3 \cdot \hat{\phi}_3^L \cdot P \quad (1)$$

where $\hat{\phi}_3^L$ is the solute fugacity coefficient in the solution (pure liquid solvent or liquid solvent plus CO₂ anti-solvent) and P is the equilibrium pressure.

The fugacity coefficient of the pure solid, $f_3^S(T, P)$, can be calculated from that of the pure liquid $f_3^L(T, P)$ as reported by Prausnitz et al.⁴¹.

In this study the Peng-Robinson equation of state (PR-EoS) was applied for the $\hat{\phi}_3^L$ calculation, with the classical Van der Waals mixing rules in

which a and b , energetic and volumetric parameters, are derived by two binary interaction parameters: k_{ij} for the attractive term and l_{ij} for the repulsive one.

The needed melting point and heat of fusion values of Quer were determined by differential scanning calorimeter, while Quer molar solid and liquid volume (v_3^S, v_3^L) were calculated by crystal unit cell data and Girolami's method⁴², respectively.

Pure component properties used in the equation of state are reported in table 2. The properties such as critical temperature (T_c), critical pressure (P_c) and the acentric factor (ω) of the organic solvents and carbon dioxide were taken from literature^{43–45}.

For Quercetin, a method described in literature⁴⁰ was used for the evaluation of critical properties and acentric factor. SAS experiments were kept at constant temperature so only one binary parameter k_{ij} was used for the correlation of the binary solubility of Quer in the different organic solvents. The same mixing rule was also applied for the binary system Quercetin-CO₂: in this case the numerical value of k_{ij} was calculated by fitting solubility values reported in literature⁴⁶.

In the case of the binary systems CO₂-organic solvent, vapour liquid equilibrium data were used for the calculation of the k_{ij} and l_{ij} parameters.

Particle size and shape analysis

Particle size and elongation factor characterizations of samples were determined using an optical microscope (Reichert Biovar, Wien, Austria) (magnification 1000 x). Small amounts of each sample were uniformly dispersed on top of a microscopy glass slide. For each powder batch, 10 microscopy glass slides were prepared, examining at least 1,800 particles per sample. Pictures were examined with the image analysis program ImageJ and the size of each sample was determined as Feret diameter while the shape factor was expressed as roundness⁴⁷.

$$Roundn = \frac{4 \text{ Area}}{\pi \cdot \text{major axis}} \quad (2)$$

Table 2 – Pure components properties

Substance	MW	T ^f (K)	ΔH^f (kJ·mol ⁻¹)	T _c (K)	P _c (bar)	ω	V ^{sol} (cm ³ ·mol ⁻¹)	V ^{liq} (cm ³ ·mol ⁻¹)	Ref.
CO ₂	44.01			304.20	73.80	0.224			43
Acetone	58.08			508.01	47.00	0.307			43
DMSO	78.13			720.00	57.05	0.350			44
EtOH	46.07			516.15	63.73	0.635			45
Quercetin	302.23	578.0	11.4	945.00	23.03	0.992	194.4	270.0	<i>This work</i>

Powder X-ray diffraction studies (PXRD)

PXRD studies were done using a STOE D500 (Siemens, Monaco, Germany) diffractometer with Cu K α radiation ($\lambda = 1.5418 \text{ \AA}$), monochromatised by a secondary flat graphite crystal. The scanning angle ranged from 3° to 40° of 2θ , steps were of 0.02° of 2θ , and the counting time was of 10 s/step. The current used was 20 mA and the voltage 40 kV.

A profile fitting based on Marquardt non-linear least squares algorithm⁴⁸ was subsequently applied to selected ranges of the data, allowing the elimination of background contributions and the separation of overlapping diffraction maxima. The values of diffracted intensity and of full width at half maximum (FWHM) for each peak, were taken from the fitted profiles to estimate the average crystallite size by means of Scherrer's equation⁴⁹:

$$D = \frac{K\lambda}{\beta \cos \theta} \quad (3)$$

Where D is the mean crystallite dimension, K is the shape factor with a typical value of 0.9, λ (CuK α 1.5418 \AA) is the X-ray wavelength, β is the line broadening value at the FWHM in radians and θ is the Bragg angle. Furosemide crystallite size was calculated from the single reflections.

ATR-Fourier Transform Mid-Infrared Spectroscopy

A FTIR mid-infrared spectrometer instrument (Bruker VERTEX 80/80 v, Ettlingen, Germany) was used to obtain spectra which comprised a KBr Beamsplitter, a diffuse reflectance absorbance scanning accessory equipped with a mercury-cadmium telluride (MCT) detector and a sampling compartment fitted with a horizontal attenuated total reflectance (HATR) sampling. An average of 30 scans for each sample were collected at 4 cm^{-1} resolution in the range $4500\text{--}600 \text{ cm}^{-1}$.

Determination of drug dissolution

Profiles of Quercetin release were obtained according to the USP 33 paddle method: 100 rpm, 900 mL of simulated gastrointestinal fluids at pH 1.2 and pH 7.4, $T = 310.1 \pm 0.1 \text{ K}$, sink conditions ($C < 0.2 \text{ Cs}$). The aqueous solution was filtered ($0.45 \mu\text{m}$ porosity) and continuously pumped to a flow cell in a spectrophotometer and absorbance were recorded at 253 and 265 nm for pH 1.2 and 7.4 respectively. Experimental points were the average of at least three replicates, and standard deviations did not exceed $\pm 5\%$ of mean value. The composition of the dissolution media was 0.2 M NaCl/0.2 M HCl (pH 1.2) or 0.2 M KH_2PO_4 /0.2 M NaOH (pH 7.4) according to USP.

Results and discussions

A temperature of 313.0 K was set in the SAS precipitation experiments. First Quer particle formations were obtained at 95.0 bar for systems with ethanol and acetone and at 102.0 bar for the system with DMSO.

In Figure 2 the behaviors of Quer-CO₂-EtOH and Quer-CO₂-DMSO ternary systems, at 313.0 K and different pressures, are presented.

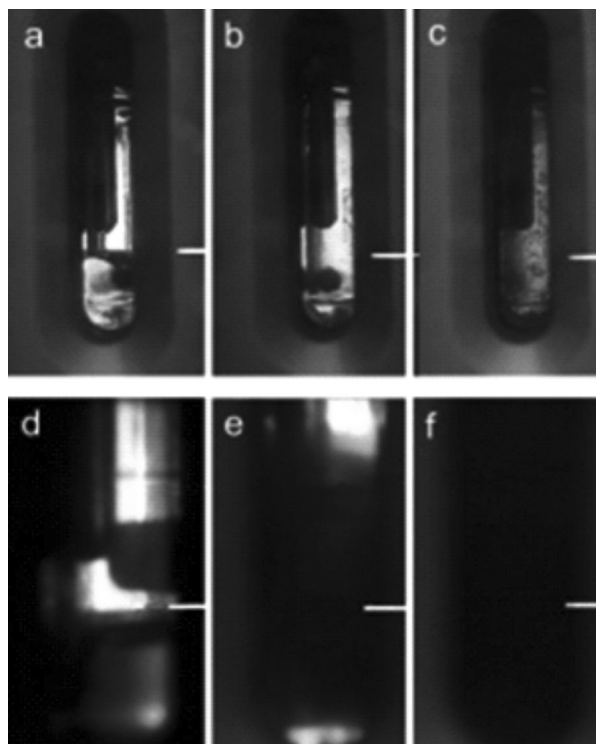


Fig. 2 – Visual cell pictures at 313.0 K of Quer in ethanol ($a = 1.0 \text{ bar}$; $b = 94.3 \text{ bar}$; $c = 97.0 \text{ bar}$) and DMSO ($d = 1.0 \text{ bar}$; $e = 102.1 \text{ bar}$; $f = 173.5 \text{ bar}$). The white line correspond to 5 mL.

Experimental conditions for the anti-solvent precipitation processes of the ternary systems were described by the Peng Robinson's Equation of State (PR-EoS), starting from binary solubility data as described previously⁴⁰; table 3 reports the values of the calculated binary interaction parameters for the different binary systems.

Starting from these binary coefficients the behavior of the different ternary systems (Quer-CO₂-organic solvent) can be predicted. Then, a three-phase equilibrium (gas-liquid-solid) has been calculated⁵² for each ternary system varying the Quer liquid phase concentration, increasing the system pressure with CO₂ addition, at temperature of 313.0 K.

Figure 3 depicts the surface area simulations of Quercetin in the studied CO₂-organic solvent mix-

Table 3 – PR-EoS binary interaction parameters

System	T (K)	$10^2 k_{ij}$	$10^2 l_{ij}$	Ref.	
Acetone	298.0	2.05	1.42	50	
	313.0	2.14	2.93	50	
CO ₂	DMSO	314.0	-0.43	-10.45	51
	EtOH	298.0	6.45	3.17	50
	313.0	8.62	-0.39	50	
	CO ₂	373.0	27.44		<i>This work</i>
	299.0	2.91		<i>This work</i>	
	DMSO	303.0	3.07		<i>This work</i>
	308.0	3.27		<i>This work</i>	
	313.0	3.46		<i>This work</i>	
	299.0	12.35		<i>This work</i>	
	Quercetin	303.0	11.97		<i>This work</i>
Acetone	308.0	11.17		<i>This work</i>	
	313.0	10.67		<i>This work</i>	
	299.0	6.94		<i>This work</i>	
	EtOH	303.0	7.27		<i>This work</i>
	308.0	7.22		<i>This work</i>	
	313.0	7.46		<i>This work</i>	

tures. In the diagrams the ordinate value c refers to the liquid Quer concentration:

$$c = \frac{mol_q}{mol_{solv} + mol_{CO_2}} \quad (4)$$

where the abscissa is the liquid CO₂ molar fraction X_{CO_2} :

$$X_{CO_2} = \frac{mol_{CO_2}}{mol_{solv} + mol_{CO_2}} \quad (5)$$

and mol_q , mol_{solv} and mol_{CO_2} are the moles of Quercetin, organic solvent and CO₂, respectively.

Then Z axis is referred to the system pressure (P).

Observing the diagrams an increase of X_{CO_2} provokes a continuous decrease of Quercetin solubility from the saturation value in the pure organic solvents. The addition of CO₂ to saturated Quercetin solutions, increases the pressure values carrying out the precipitation of Quer: in all the cases the PR-EoS can describe the precipitation ranges, confirming the experimental behaviors.

In the diagrams, the changes of gray tonality suggest the different action of CO₂, that entails both co-solvent (light gray) and anti-solvent (dark gray)

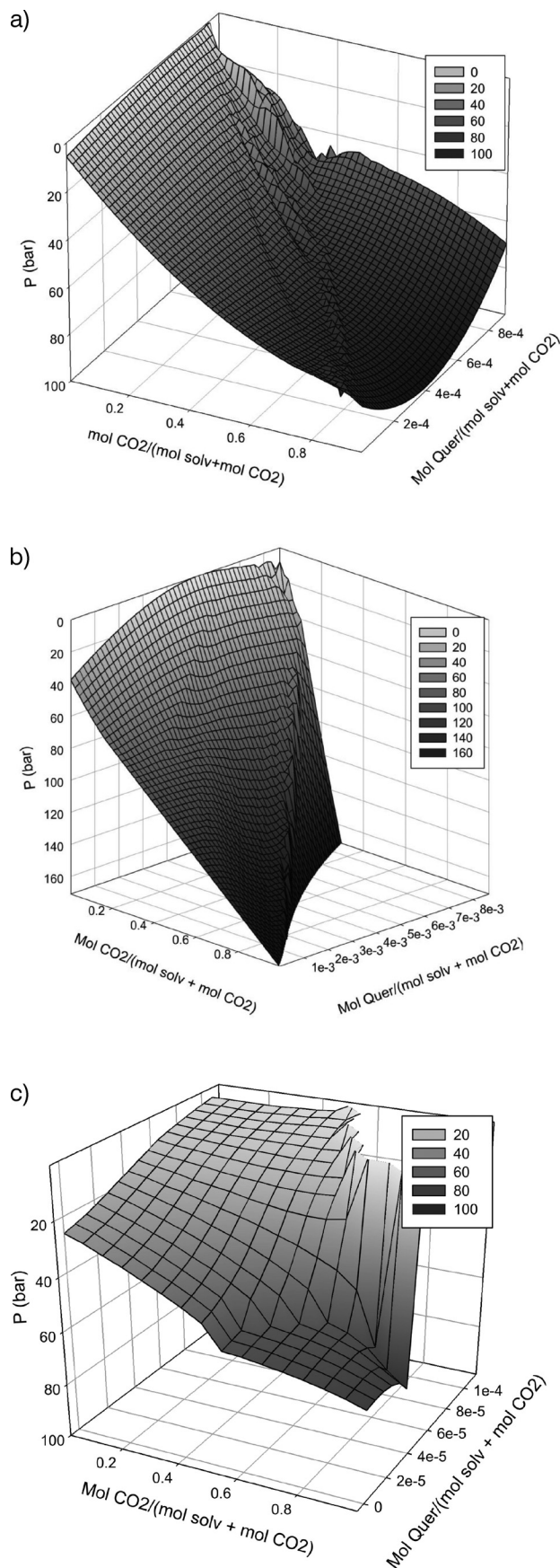


Fig. 3 – Model description of Quer-CO₂-organic solvent ternary system at 313.0 K. a) EtOH, b) DMSO, c) Acetone

effects: then darker zones are related to the particle precipitations, with pressure values close to 80 bar for EtOH and acetone systems and 115 bar for DMSO system. These results, obtained from the model based only on binary interaction coefficients, are satisfactory, giving a good agreement with the SAS experiments in which were observed precipitation of drug particles at about 95 bar in the systems with EtOH or acetone and 102 bar for the system with DMSO.

To obtaining the elimination of the organic solvent and the recovery of dry particles, and considering the experimental evidence, the SAS apparatus was then employed in dynamic way at 105.0 bar and 313.0 K.

Comparing the experimental outcomes of the three ternary systems, Quer-CO₂-EtOH reported the best behavior. In fact, due to the high density of DMSO, the Quer-CO₂-DMSO system exhibited longer times in the recovery of dry particles while, the low Quer solubility in Acetone achieved lower yields in SAS precipitation. For these reasons, the particles precipitated with Ethanol at 105.0 bar and 313.0 K were selected for the following physico-chemical characterizations.

The SAS precipitation of Quer from ethanol (Quer-EtOH) gave a very fluffy and voluminous powder.

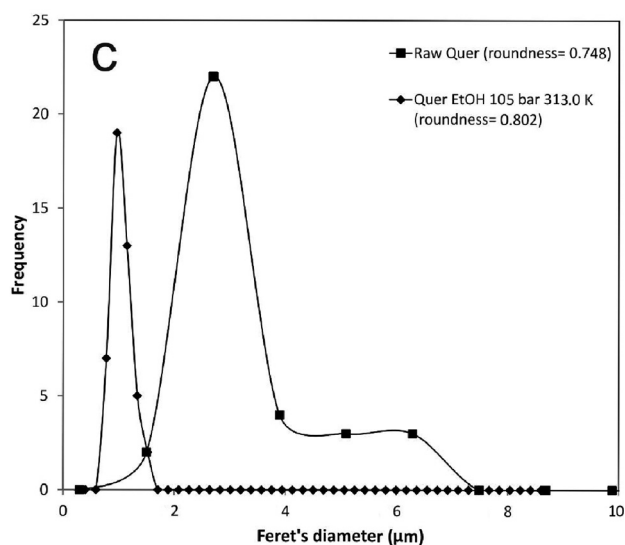
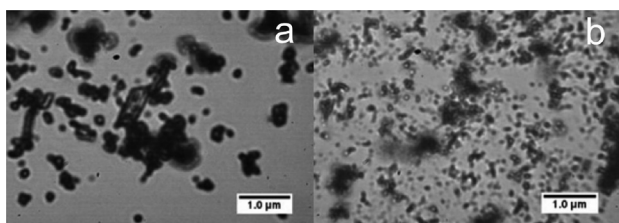


Fig. 4 – Microphotographs (magnification 1000x) of (a) Raw Quercetin and (b) Quer-EtOH precipitated at 105.0 bar and 313.0 K. (c) Particle size distributions

Figure 4, shows the precipitated Quercetin particles highlighting a reduction of their size in comparison with the raw one.

Powder diffraction patterns of Quer-EtOH in comparison with the Raw one were also investigated in order to understand the effect of SAS technique on the Quer solid state (Figure 5).

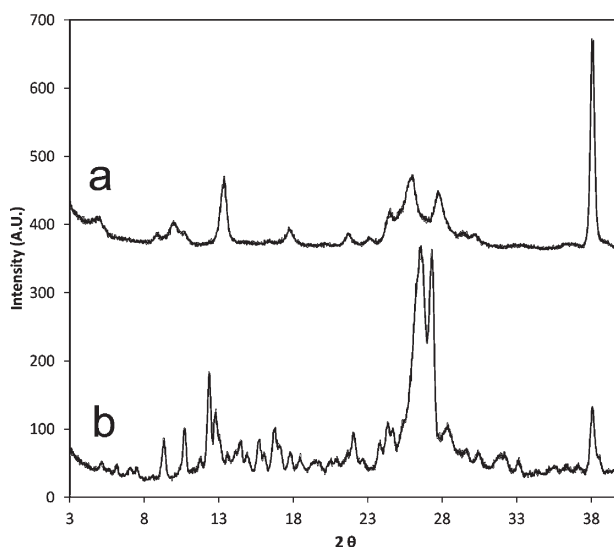


Fig. 5 – Powder diffraction patterns of (a) Quer-EtOH (105.0 bar, 313.0 K) and (b) Raw Quercetin

The X-ray analysis highlighted a different pattern for the treated Quer that should be ascribed to the dehydration of Quercetin dihydrate.

This seems to be in agreement with the FTIR spectra in which it is possible to notice two slightly different spectra (Figure 6) between the Raw and the treated Quercetin. FTIR of Raw Quercetin shows the typical spectra of dihydrate form with a broad phenolic OH band centered around 3400 cm⁻¹,

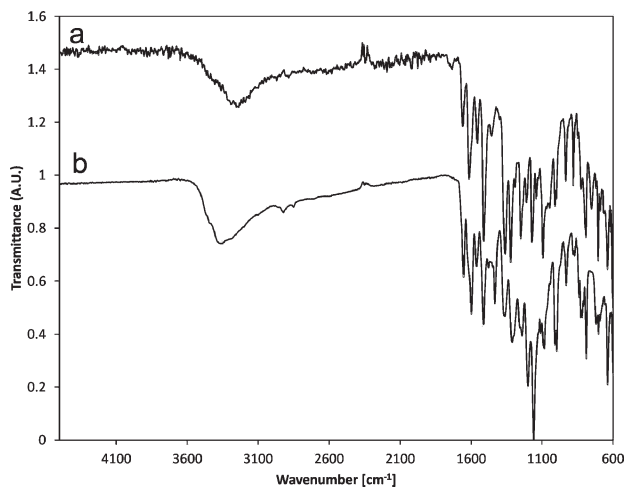


Fig. 6 – FTIR spectra of (a) Quer-EtOH (105.0 bar, 313.0 K) and (b) Raw Quercetin

characteristic --CO stretching at 1654 cm^{-1} , aromatic bending and stretching around 1100 and 1600 cm^{-1} , --OH phenolic bending around 1200 and 1400 cm^{-1} . Quer-EtOH, instead, shows a shift of the phenolic OH band at about 3280 cm^{-1} and a slight moving to higher values for --CO stretching and aromatic bending peaks. Changes in --OH phenolic bending were also noticed. These shifts could be ascribed to the loss in water from the structure as reported in literature⁵³. Nevertheless, also these aspects will be better investigated.

X-ray analysis was adopted also to estimate the crystallite size of the considered systems. By means of Sherrer's equation it is possible to infer the strong reduction in crystallite size for Quer-EtOH respect to the Raw Quer as reported in Table 4.

Table 4 – Crystallite size of considered samples

Sample	Crystallite size (nm)
Raw Quer	40.9 ± 7.0
Quer-EtOH (105.0 bar, 313.0 K)	22.5 ± 1.5

The influence of SAS technique on Quercetin solid state was also evaluated through the dissolution behaviors in the simulated gastrointestinal fluids. It must be pointed out that the Quercetin solubility is pH dependence showing values of $6.9 \pm 0.6\text{ }\mu\text{g mL}^{-1}$ and $28 \pm 1.15\text{ }\mu\text{g mL}^{-1}$ respectively at pH 1.2 and 7.4 at 310.1 K confirming the literature values⁵⁴.

The dissolution behaviors of Quer-EtOH show the best dissolution profile in both pH medium respects to the Raw Quercetin (Figure 7). This issue highlights, even in this case, how the particle and the crystallite size reduction play an important role, favoring the increase in surface area of the drug and carrying to an improvement of the dissolution kinetics.

Conclusion

In this work a predictive method for the evaluation of the ternary behavior on the basis of binary information is applied. The results obtained for different systems are encouraging since they highlight the essential features of the behavior of these systems. Peng–Robinson EoS was used to represent solute–solvent–antisolvent systems and it was able to predict ternary behaviors using binary interaction parameters.

The obtained particles were physicochemically characterized in order to understand the influence of the SAS technique on the drug solid state. Among the different polymorphic form of Quercetin as-

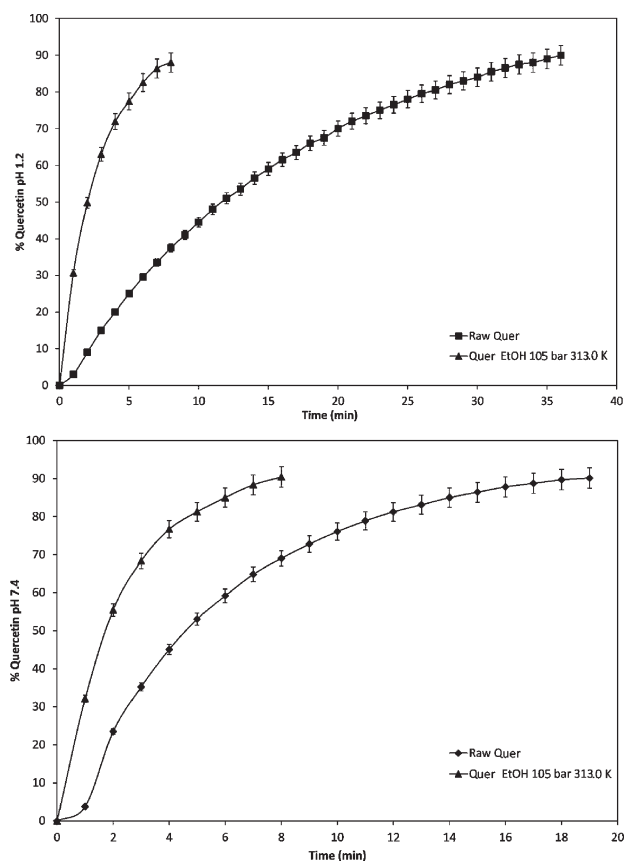


Fig. 7 – Dissolution performance of considered systems at pH 1.2 and pH 7.4

cribed to the structural water loss, SAS technique carried to the formation of finest and voluminous particles than those of the Raw Quercetin. This great increase in its surface area and decrease of crystallite size permitted the better dissolution of the considered active compound in the both simulated medium.

ACKNOWLEDGEMENTS

The authors are very grateful to Kathleen Foreman Casali Foundation (Trieste-Italy) for its financial support.

References

- Kuhnau, J., *World Rev. Nutr. Diet.* **24** (1976) 117.
- Morand, C., Crespy, V., Manach, C., Besson, C., Demigne, C., Remesy, C., *Am. J. Physiol. Regul. Integr. Comp. Physiol.* **275** (1998) R212.
- Wiczowski, W., Nemeth, K., Bucinski, A., Piskula, M.K., *Pol. J. Food Nutr. Sci.* **12** (2003) 95.
- Hertog, M.G.L., Hollman, P.C.H., Peter, C.H., Katan, M.B., *J. Agric. Food Chem.* **40** (1992) 2379.
- Day, A.J., Williamson, G., *Basic Life Sci.* **66** (1999) 415
- Harnly, J.M., Doherty, R.F., Beecher, G.R., Holden, J.M., Haytowitz, D.B., Bhagwat, S., Gebhardt, S., *J. Agric. Food Chem.* **54** (2006) 9966.

7. Hertog, M.G.L., Hollman, P.C.H., van de Putte, B., J. Agric. Food Chem. **41** (1993) 1242.
8. Sampson, L., Rimm, E., Hollman, P.C., de Vries, J.H., Katan, M.B. 2002. *J. Am. Diet Assoc.* **102** (2002) 1414.
9. Hertog, M.G.L., Kromhout, D., Aravanis, C., Blackburn, H., Buzina, R., Fidanza, F., Giampaoli, S., Jansen, A., Menotti, A., Nedeljkovic, S., Pekkarinen, M., Simic, B.S., Toshima, H., Feskens, E.J.M., Hollman, P.C.H., Katan, M.B., *Arch. Intern. Med.* **155** (1995) 381.
10. Rimm, E.C., Katan, M.B., Ascherio, A., Stampfer, M.J., Willett, W.C., *Ann. Intern. Med.* **125** (1996) 384.
11. Knekt, P., Jarvinen, R., Seppanen, R., Heliövaara, M., Teppo, L., Pukkala, E., Aromaa, A., *Am. J. Epidemiol.* **146** (1997) 223.
12. Kimira, M., Arai, Y., Shimoi, K., Watanabe, S., *J. Epidemiol.*, **8** (1998) 168.
13. Johannot, L., Somers, S.M., *Public Health Nutr.* **9** (2006) 1045.
14. Kobori, M., Masumoto, S., Akimoto, Y., Oike, H. C., *Mol. Nutr. Food Res.*, **55** (2011) 530.
15. Harwood, M., Danielewska-Nikiel, B., Borzelleca, J. F., Flamm, G. W., Williams, G.M., Lines, T.C., *Food Chem. Toxicol.* **45** (2007) 2179.
16. de Boer, V. C., Dihal, A. A., van der Woude, H., Arts, I. C. Wolffram, S., Alink, G.M., Rietjens, I.M.C.M., Kaijser, J., Hollman, P.C.H. *J. Nutr.* **135** (2005) 1718.
17. Hörter, D., Dressman, J. B., *Adv. Drug Del. Rev.* **46** (2001) 75.
18. Abu Serajuddin, T.M., *Adv. Drug Del. Rev.* **59** (2007) 603.
19. Rasenack, N., Steckel, H., Müller, B.W., *Pow. Tech.* **143–144** (2004) 291.
20. Ma, Z., Moulton, B., *Coord. Chem. Rev.* **255** (2011) 1623.
21. Morissette, S.L., Almarsson, Ö., Peterson, M.L., Remenar, J.F., Read, M.J., Lemmo, A. V., Ellis, S., Cima, M.J., Gardner, C.R., *Adv. Drug Del. Rev.* **56** (2004) 275.
22. Bundgaard, H., Buur, A., Hansen, K.T., Larsen, J.D., Møss, J., Olsen, L., *Int. J. Pharm.* **45** (1988) 47.
23. Thirawong, N., Thongborisute, J., Takeuchi, H., Sriamornsak, P., *J. Control. Rel.* **125** (2008) 236.
24. Gupta, M.K., Vanwert, A., Bogner, R.H., *J. Pharm. Sci.* **92** (2003) 536.
25. Grant, N., Zhang, H., *J. Colloid Inter. Sci.* **356** (2011) 573.
26. Gonnissen, Y., Verhoeven, E., Peeters, E., Remon, J.P., Vervaet, C., *Eur. J. Pharm. Biopharm.* **69** (2008) 320.
27. Moneghini, M., Perissutti, B., Vecchione, F., Kikic, I., Alessi, P., Cortesi, A., Princivalle, F., *Curr. Drug Deliv.* **4** (2007) 241.
28. De Zordi, N., Kikic, I., Moneghini, M., Solinas, D., *J. Supercrit. Fluids* **55** (2010) 340.
29. De Zordi, N., Moneghini, M., Kikic, I., Grassi, M., Del Rio Castillo, A.E., Solinas, D., Bolger, M.B., *Eur. J. Pharm. Biopharm.* **81** (2012) 131.
30. Kalani, M., Yunus, R., *Int. J. Nanomed.* **6** (2011) 1429.
31. Cocero, M.M.J., Mattea, F., Varona, S., *J. Supercrit. Fluids* **47** (2009) 546.
32. Fages, J., Lochard, H., Letourneau, J.J., Sauceau, M., Rodier, E., *Pow. Tech.* **141** (2004) 219.
33. Reverchon, E., Adami, R., Caputo, G., De Marco, I., *J. Supercrit. Fluids* **47** (2008) 70.
34. Reverchon, E., Adami, R., *J. Supercrit. Fluids* **37** (2006) 1.
35. Yeo, S.D., Kiran, E., *J. Supercrit. Fluids* **34** (2005) 287.
36. Jung, J., Perrut, M., *J. Supercrit. Fluids* **20** (2001) 179.
37. Reverchon, E., Caputo, G., De Marco, I., *Ind. Eng. Chem. Res.* **42** (2003) 6406.
38. Kikic, I., Vecchione, F., *Cur. Opinion Solid State Mat. Sci.* **7** (2003) 399.
39. Chen, A.-Z., Li, Y., Chau, F.-T., Lau, T.-Y., Hu, J.-Y., Zhao, Z., Mok, D.K., *J. Supercrit. Fluids* **49** (2009) 394.
40. Kikic, I., De Zordi, N., Moneghini, M., Solinas, D., *J. Supercrit. Fluids* **55** (2010) 616.
41. Prausnitz, J.M., Lichtenthaler, R.N., de Azevedo, E.G. *Molecular Thermodynamics of Fluid Phase Equilibria*, third ed., Prentice-Hall, Englewood Cliffs, NJ, 1999.
42. Girolami, G.S. *J. Chem. Educ.* **71** (1994) 962.
43. Poling, B., Prausnitz, J.M., O'Connell, J.P. *The Properties of Gases and Liquids*, 5th ed., McGrawHill, New York, 2004
44. Kordikowsky, A., Schenk, A. P., Van Nielen, R. M., Peters, C. J., *J. Supercrit. Fluids* **8** (1995) 205.
45. Reverchon, E., Della Porta, G., Taddeo, R., Pallado, P., Stassi, A., *Ind. Eng. Chem. Res.* **34** (1995) 4087.
46. Chafer, A., Fornari, T., Berna, A., Stateva, R.P., *J. Supercrit. Fluids* **32** (2004) 89.
47. Rasband, W.S., ImageJ, U. S. National Institutes of Health, Bethesda, Maryland, USA, <http://rsb.info.nih.gov/ij/>, 1997–2005
48. Schreiner, W.N., Jenkins, R., *Adv. X-ray Anal.* **26** (1983) 141.
49. Patterson, A., *Phys. Rev.* **56** (1939) 978.
50. Day, C., Chang, C. J., Chen, C., *J. Chem. Eng. Data*, **44** (1999) 365.
51. Vega Gonzales, A., Tufeu, R. S. P., *J. Chem. Eng. Data*, **47** (2002) 492.
52. Colussi, S., Elvassore, N., Kikic, I., *J. Supercrit. Fluids*, **38** (2006) 18.
53. Koradia, V., Lopez De Diego, H., Frydenvang, K., Ringkjøbing-Elema, M., Müllertz, A., Bond, A. D., Rantanen, J., *Cryst. Growth Des.*, **10** (2010) 5279.
54. Li, H., Zhao, X., Ma, Y., Zhai, G., Li, L., Lou, H., *J. Control. Release*, **133** (2009) 238.